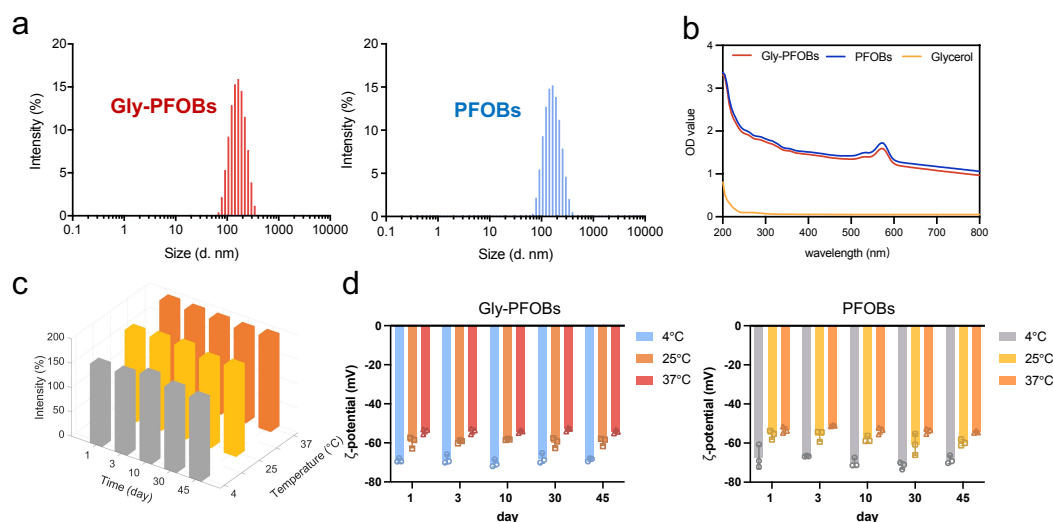


## Supplementary information



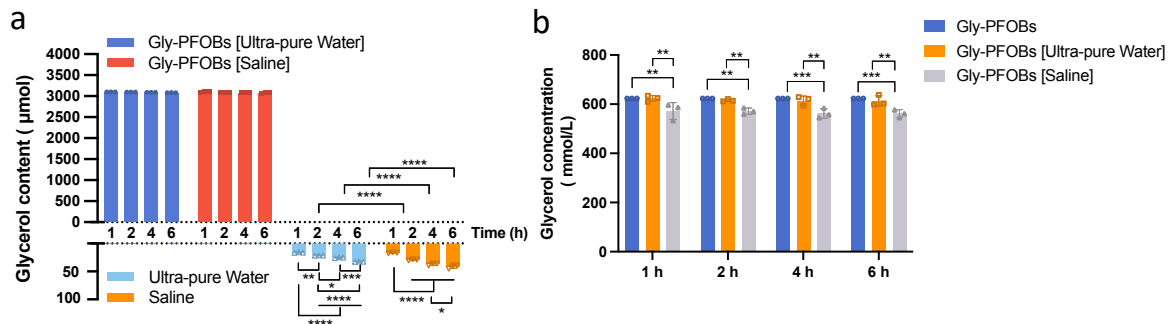
**Supplementary Figure 1. Characteristics of Gly-PFOBs and PFOBs.** a. Hydrodynamic particle sizes of Gly-PFOBs and control probe without CEST signals (PFOBs) were characterized by DLS. Repeated 4 times independently with similar results. b. Corresponding UV-VIS spectra of glycerol, Gly-PFOBs, and PFOBs. Repeated 4 times independently with similar results. c. Measurement of changes in the intensity-averaged mean particle size (hydrodynamic particle diameter) of PFOBs (n=5 independent measurements). Three-dimensional (3D) graphs were generated using Matlab based on the average values obtained. d Measurement of changes in the zeta potential of CESTs and PFOBs at 4 °C, 25 °C, and 37 °C within 45 days (n=3 independent measurements).

<i>Duration</i>	<i>Gly-PFOBs dialyzed against ultra-pure water(<math>\mu\text{mol}</math>)</i>	<i>Ultra-pure water(<math>\mu\text{mol}</math>)</i>	<i>Gly-PFOBs dialyzed against saline (<math>\mu\text{mol}</math>)</i>	<i>Saline (<math>\mu\text{mol}</math>)</i>
<i>1 h</i>	$3099 \pm 0.59$	$16.04 \pm 0.59$	$3098 \pm 0.84$	$16.74 \pm 0.84$
<i>2 h</i>	$3094 \pm 0.38$	$21.43 \pm 0.38$	$3086 \pm 0.87$	$29.14 \pm 0.87$
<i>4 h</i>	$3090 \pm 0.86$	$25.23 \pm 0.86$	$3078 \pm 1.8$	$37.16 \pm 1.80$
<i>6 h</i>	$3083 \pm 0.39$	$32.30 \pm 0.39$	$3074 \pm 3.3$	$41.43 \pm 3.25$

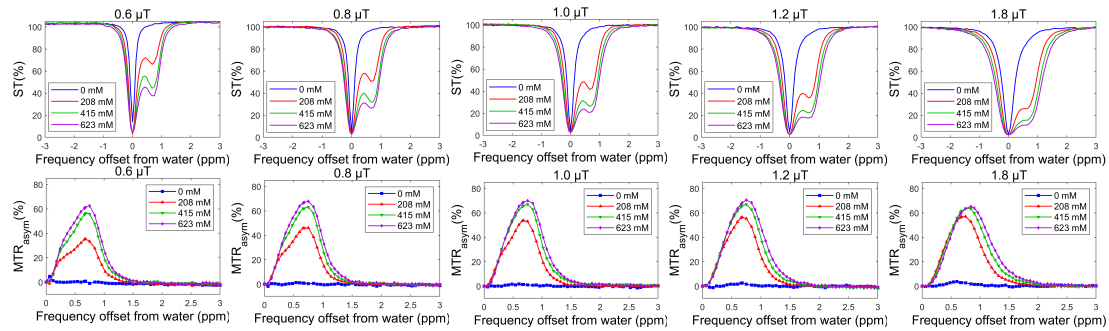
**Supplementary Table 1.** The glycerol content in Gly-PFOBs and in different dialysates (ultra-pure water or saline) at different time points were determined by Free Glycerol Assay Kit (abcam), n=3 independent samples.

Duration	Gly-PFOBs without dialysis	Gly-PFOBs dialyzed against Ultra-pure water (mmol/L)	Gly-PFOBs dialyzed against Saline (mmol/L)
1 h	623.51 ± 39.42	622.93 ± 12.18	572.44 ± 33.97
2 h		615.39 ± 4.87	571.62 ± 12.72
4 h		614.64 ± 18.42	562.21 ± 20.13
6 h		612.96 ± 21.5	561.51 ± 15.83

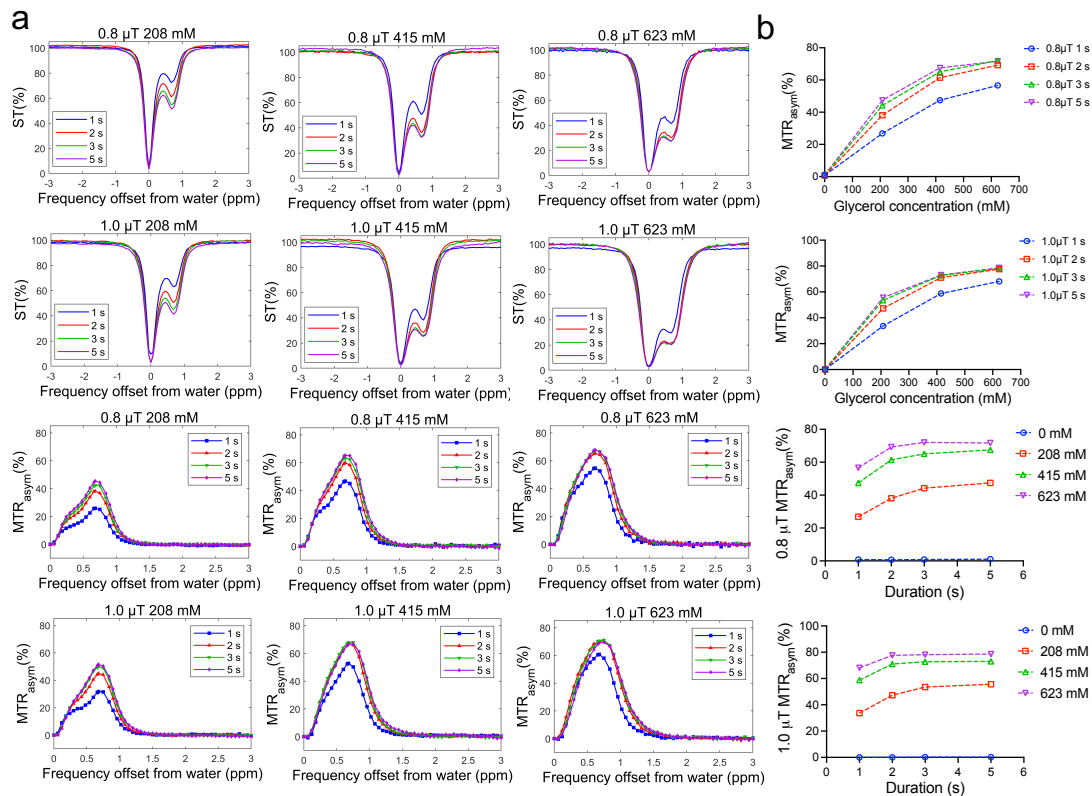
**Supplementary Table 2.** The glycerol concentration in Gly-PFOBs without dialysis and glycerol concentration in Gly-PFOBs dialyzed against different dialysates (ultra-pure water or saline) at different time points were determined by Gas Chromatography/Mass Spectrometry (GC/MS) analysis, n=3 independent samples.



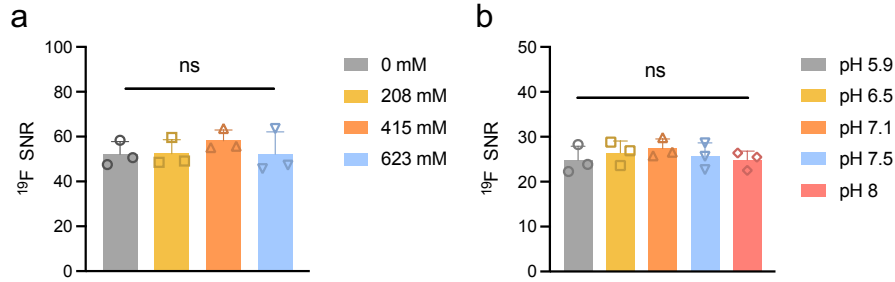
**Supplementary Figure 2. Evaluation of the persistence of glycerol component on the Gly-PFOBs.** a. The glycerol content in Gly-PFOBs and different dialysate (ultra-pure water or saline) at different time points was determined by Free Glycerol Assay Kit (abcam), \*  $P=0.0242$ , glycerol in ultra pure water (dialysate) 2 h vs. 4 h; \*  $P=0.0110$ , glycerol in saline 4 h vs. 6 h, \*\*  $P=0.0016$ , glycerol in ultra pure water (dialysate) 1 h vs. 2 h, \*\*\*  $P=0.0001$ , glycerol in ultra pure water (dialysate) 4 h vs. 6 h, \*\*\*\*  $P < 0.0001$ , two-way ANOVA, Tukey's multiple comparisons test; b. Gas Chromatography-Mass Spectrometry (GC-MS) analysis was performed to determine glycerol concentrations in Gly-PFOBs after different duration of dialysis (1 h, 2 h, 4 h, 6 h). \*\*  $P=0.0017$ , Gly-PFOBs 1 h vs. Gly-PFOBs [Saline] 1 h, \*\*  $P=0.0014$ , Gly-PFOBs [Ultra-pure water] 1 h vs. Gly-PFOBs [Saline] 1 h; \*\*  $P=0.0061$ , Gly-PFOBs 2 h vs. Gly-PFOBs [Saline] 2 h, \*\*  $P=0.0017$ , Gly-PFOBs [Ultra-pure water] 2 h vs. Gly-PFOBs [Saline] 2 h; \*\*\*  $P=0.0002$ , Gly-PFOBs 4 h vs. Gly-PFOBs [Saline] 4 h, \*\*  $P=0.0011$ , Gly-PFOBs [Ultra-pure water] 4 h vs. Gly-PFOBs [Saline] 4 h; \*\*\*  $P=0.0002$ , Gly-PFOBs 6 h vs. Gly-PFOBs [Saline] 6 h, \*\*  $P=0.0014$ , Gly-PFOBs [Ultra-pure water] 6 h vs. Gly-PFOBs [Saline] 6 h, two-way ANOVA, Tukey's multiple comparisons test. Data are presented as mean ± standard deviation (SD) (n = 3 independent samples).



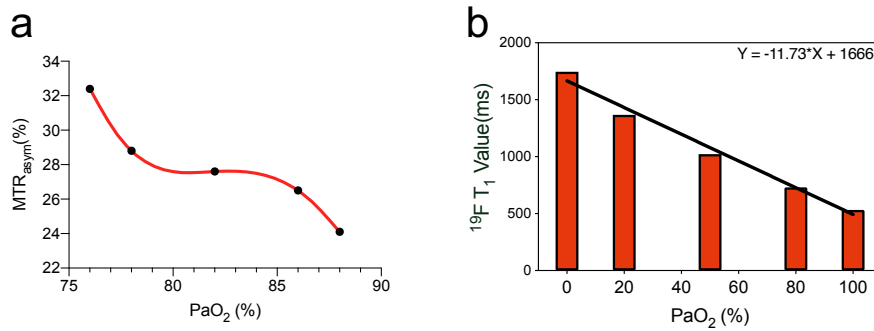
**Supplementary Figure 3. CEST signal properties of Gly-PFOBs.** Z-Spectra and  $MTR_{\text{asym}}(\%)$  curve of Gly-PFOBs containing different concentrations (0 mM, 208 mM, 425 mM, and 623 mM) of glycerol at different saturation pulse powers (0.6  $\mu\text{T}$ , 0.8  $\mu\text{T}$ , 1.0  $\mu\text{T}$ , 1.2  $\mu\text{T}$ , and 1.8  $\mu\text{T}$ ) with same saturation pulse duration (5s). The experiment was repeated  $n=3$  times with similar results.



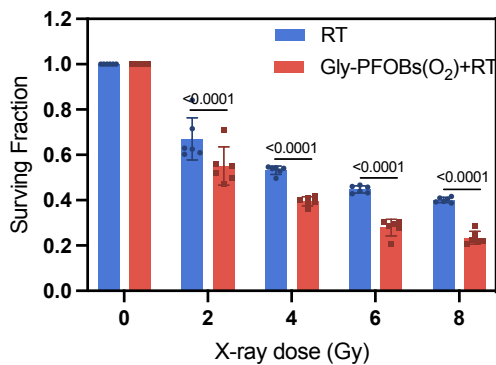
**Supplementary Figure 4. CEST signal properties of Gly-PFOBs.** a. Z-Spectra and  $MTR_{\text{asym}}$  curve of Gly-PFOBs containing different concentrations (0 mM, 208 mM, 425 mM, and 623 mM) of glycerol at different saturation pulse durations (1 s, 2 s, 3 s, and 5 s) and different saturation pulse powers (0.8  $\mu\text{T}$  and 1.0  $\mu\text{T}$ ), and b. corresponding statistical analysis. The experiment was repeated  $n=3$  times with similar results.



**Supplementary Figure 5. Statistical results of  $^{19}\text{F}$ -MRI signal-to-noise ratio (SNR) of the phantom.** a.  $^{19}\text{F}$ -MRI SNR statistical results of Gly-PFOBs with different glycerol concentrations b.  $^{19}\text{F}$ -MRI SNR statistical results of Gly-PFOBs in different pH solutions. n. s., no significance, one-way ANOVA, Tukey's multiple comparisons test. Data are presented as mean  $\pm$  standard deviation (SD) (n = 3 independent samples).

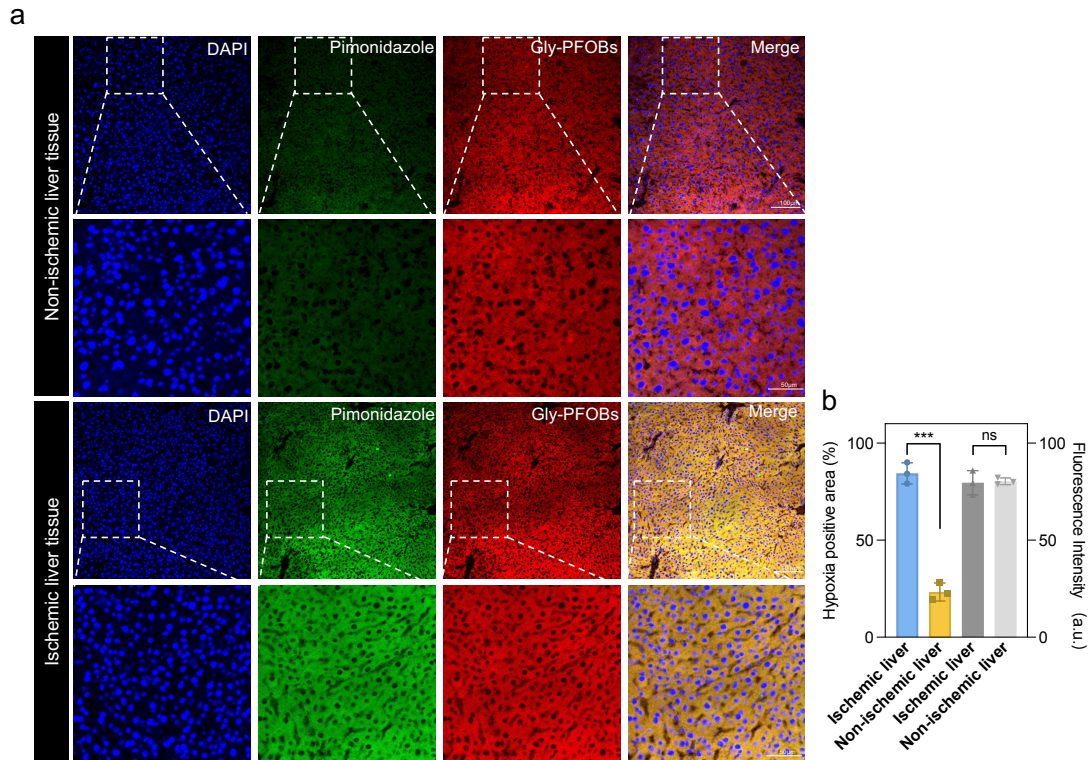


**Supplementary Figure 6.  $^{19}\text{F}/^1\text{H}$ -CEST signal properties of Gly-PFOBs under different oxygen partial pressure.** a. CEST signal intensity of Gly-PFOBs under different oxygen partial pressure. b.  $^{19}\text{F}$  T<sub>1</sub> value of Gly-PFOBs under different oxygen partial pressure. MTR<sub>asymp</sub>: magnetization transfer ratio asymmetry. a-b. Repeated 3 times independently with similar results.

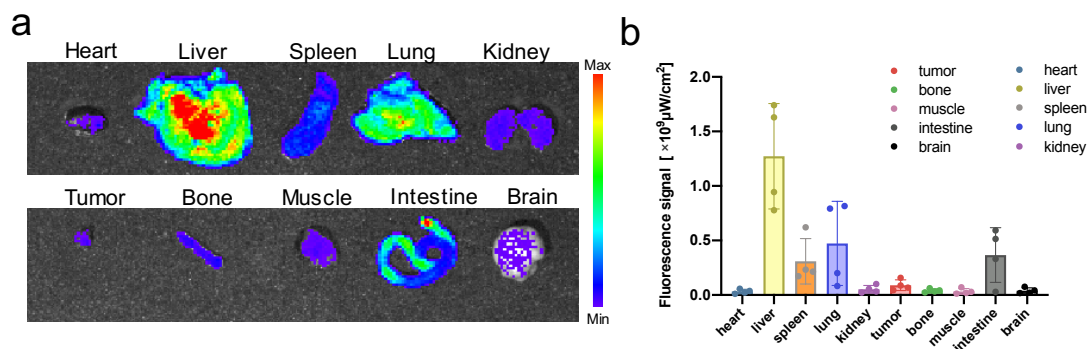


**Supplementary Figure 7. Cell viability.** Hypoxic cell viability results at different X-ray radiation doses (0 Gy, 2 Gy, 4 Gy, 6 Gy, or 8 Gy) in the presence of Gly-PFOBs (O<sub>2</sub>). \*\*\*\*  $P < 0.0001$ , n = 6 independent measurements, Two-way ANOVA, Sidak's multiple comparisons test. Data are presented as mean  $\pm$  standard deviation (SD). RT: radiotherapy.

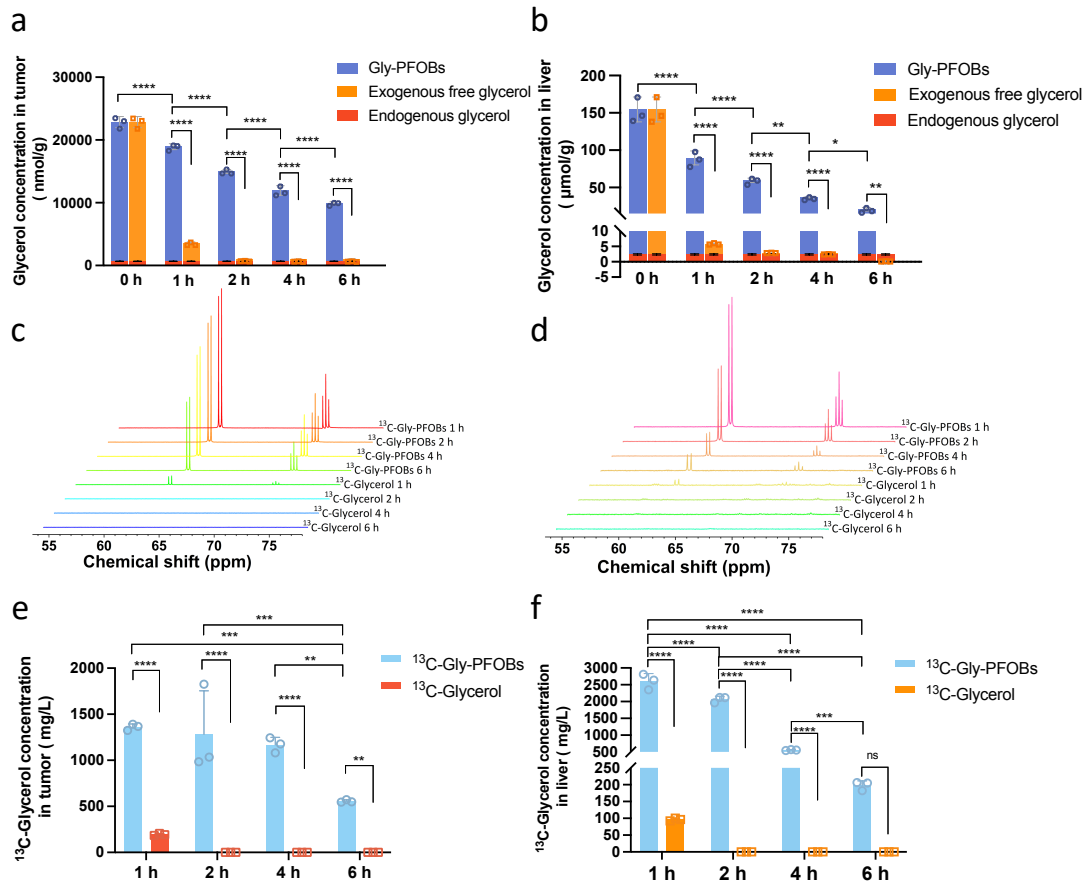




**Supplementary Figure 8. Immunofluorescence results of hypoxia staining and Gly-PFOBs in liver.** a. Immunofluorescence results of pimonidazole hydrochloride and rhodamine B labeled Gly-PFOBs in the ischemic and non-ischemic liver, and b. corresponding statistical results. \*\*\*  $P = 0.0001$ , n. s., no significance. Two-tailed, unpaired t-test.  $n = 3$  independent experiments. Scale bar: 100  $\mu\text{m}$  (scale bar for magnified micrograph, 50  $\mu\text{m}$ ). Data are presented as mean  $\pm$  standard deviation (SD).

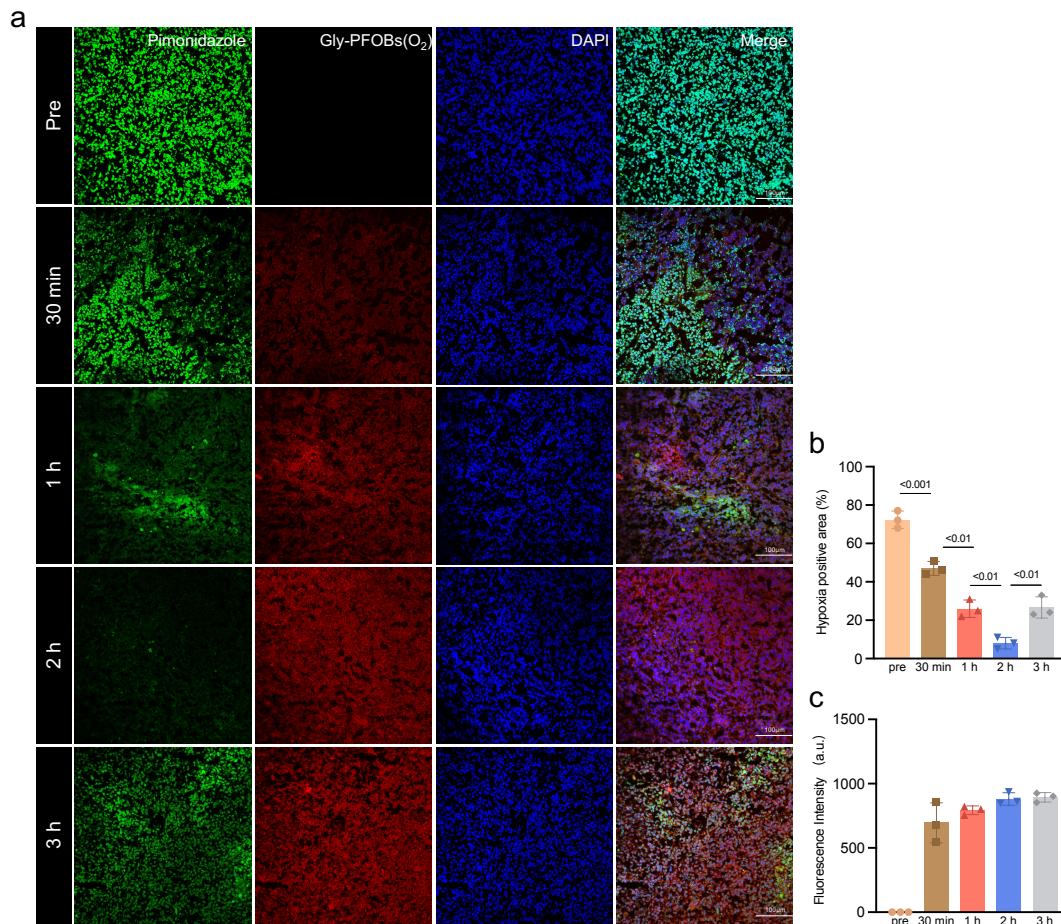


**Supplementary Figure 9. Biodistribution of Gly-PFOBs in NCI-H460 tumor bearing mouse model.** a. Average fluorescence intensity biodistribution percentage of tumor and major organs after intravenous injection of Gly-PFOBs, and b. corresponding *ex vivo* fluorescence analysis ( $n = 4$  mice). Data are presented as mean  $\pm$  standard deviation (SD).

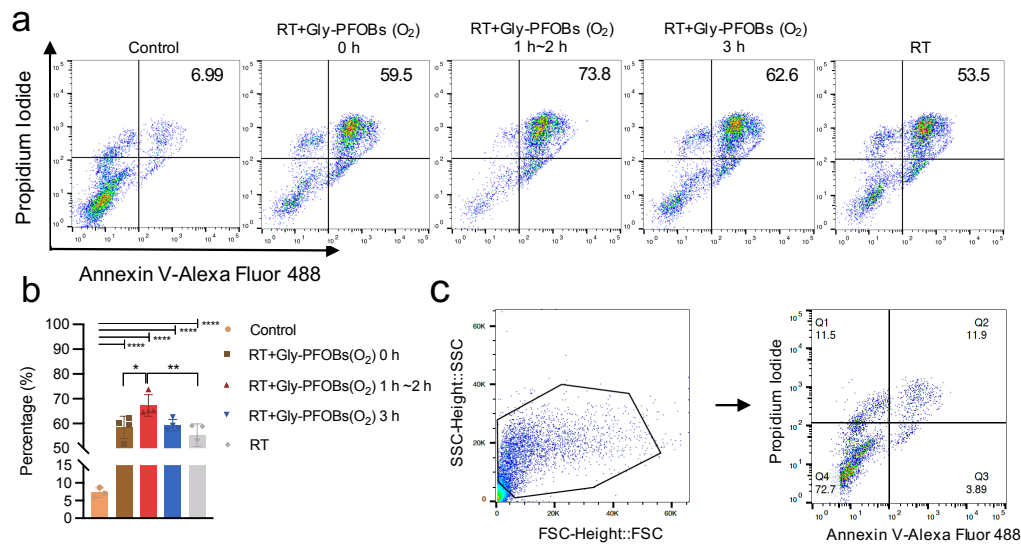


**Supplementary Figure 10. The determination of *in vivo* glycerol retaining status of Gly-PFOBs in subcutaneous tumor or liver tissue.** a. The glycerol concentration in tumor tissue was determined by Free Glycerol Assay Kit at different time points after intratumoral injection of Gly-PFOBs or free glycerol containing same amount of glycerol (623 mM based on glycerol, 50  $\mu$ l). Meanwhile, the concentration of endogenous glycerol in tumor was also quantified for accurately reflect the exogenous glycerol concentration. \*\*\*\*  $P < 0.0001$ ,  $n = 3$  independent samples. Two-way ANOVA, Tukey's multiple comparisons test; b. The glycerol concentration in liver tissue was determined by Free Glycerol Assay Kit (Abcam, ab65337) at different time points after intravenous injection of Gly-PFOBs or free glycerol containing same amount of glycerol (623mM based on glycerol, 200  $\mu$ l). The concentration of endogenous glycerol in tumor was also quantified. \*  $P = 0.0472$ ; \*\* $P = 0.0016$ , Gly-PFOBs 2 h vs. Gly-PFOBs 4 h; \*\* $P = 0.0047$ , Gly-PFOBs 6 h vs. Exogenous free glycerol 6 h; \*\*\*\*  $P < 0.0001$ ;  $n = 3$  independent samples. Two-way ANOVA, Tukey's multiple comparisons test. c and e. <sup>13</sup>C-NMR (c), GC-MS (e) analysis was performed to determine the metabolic tendency or concentration of <sup>13</sup>C-glycerol in NCI-H460 tumor tissue at different time points after intratumoral injection of <sup>13</sup>C-Gly-PFOBs or free <sup>13</sup>C-glycerol containing same amount of <sup>13</sup>C-glycerol (623mM based on <sup>13</sup>C-glycerol, 50  $\mu$ l), <sup>13</sup>C-glycerol inherently showed two characteristic peaks at 62.5 ppm and three characteristic peaks at 72 ppm; d and f. <sup>13</sup>C-NMR (d), GC-MS (f) analysis was used to determine the metabolic tendency or concentration of <sup>13</sup>C-glycerol in liver tissue at different time

points after intratumoral injection of  $^{13}\text{C}$ -Gly-PFOBs or free  $^{13}\text{C}$ -glycerol containing same amount of  $^{13}\text{C}$ -glycerol (623 mM based on  $^{13}\text{C}$ -glycerol, 200  $\mu\text{l}$ ). *P* values in (e): \*\*  $P=0.0027$ ,  $^{13}\text{C}$ -Gly-PFOBs 4 h vs.  $^{13}\text{C}$ -Gly-PFOBs 6 h; \*\*\*  $P=0.0002$ ,  $^{13}\text{C}$ -Gly-PFOBs 1 h vs.  $^{13}\text{C}$ -Gly-PFOBs 6 h; \*\*\*  $P=0.0005$ ,  $^{13}\text{C}$ -Gly-PFOBs 2 h vs.  $^{13}\text{C}$ -Gly-PFOBs 6 h; \*\*  $P=0.0041$ ,  $^{13}\text{C}$ -Gly-PFOBs 6 h vs.  $^{13}\text{C}$ -Glycerol 6 h, Two-way ANOVA, Sidak's multiple comparisons test,  $n = 3$  independent samples. *P* values in (f): \*\*\*  $P=0.0008$ ,  $^{13}\text{C}$ -Gly-PFOBs 4 h vs.  $^{13}\text{C}$ -Gly-PFOBs 6 h; \*\*\*\*  $P < 0.0001$ ; n. s., no significance, Two-way ANOVA, Sidak's multiple comparisons test,  $n = 3$  independent samples. Data are presented as mean  $\pm$  standard deviation (SD).

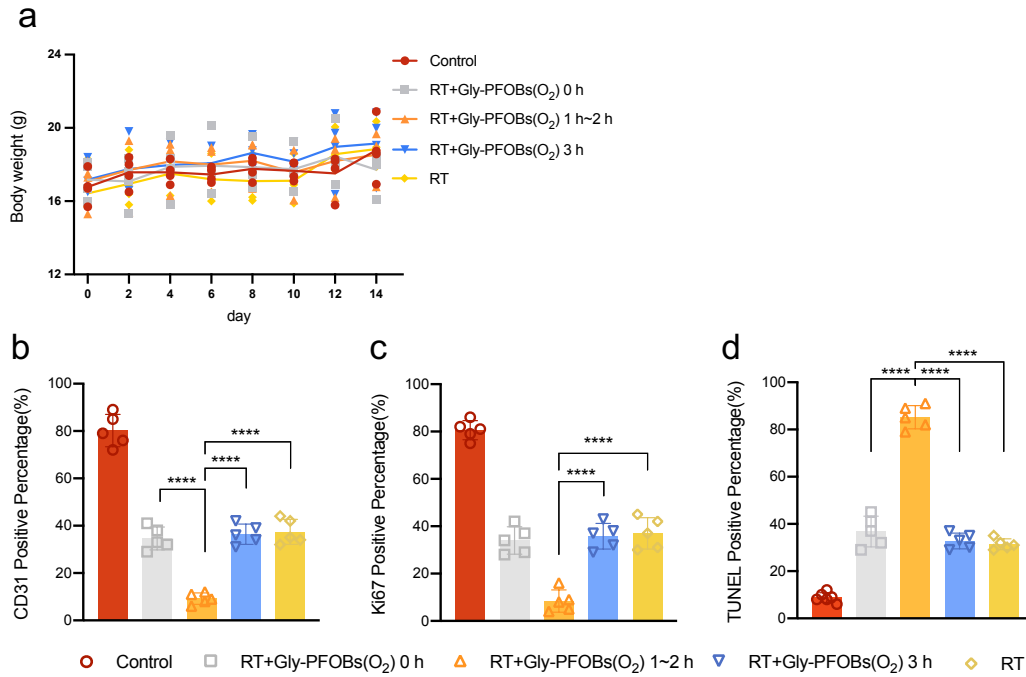


**Supplementary Figure 11. Pimonidazole hydrochloride immunofluorescence staining results.** a. Representative pimonidazole hydrochloride immunofluorescence staining results of NCI-H460 tumor tissues at different time points before and after intra-tumoral injection of rhodamine B-labeled Gly-PFOBs (O<sub>2</sub>) b. corresponding statistical analysis of hypoxia positive area and c. fluorescence intensity of Gly-PFOBs. \*\*\*  $P=0.0002$ , pre vs. 30 min, \*\*  $P=0.0010$ , 30 min vs. 1 h, \*\*  $P=0.0013$ , 30 min vs. 3 h, \*\*  $P=0.0033$ , 1 h vs. 2 h, \*\*  $P=0.0025$ , 2 h vs. 3 h, one-way ANOVA, Tukey's multiple comparisons test,  $n = 3$  independent experiments. Scale bar: 100  $\mu\text{m}$ . Data are presented as mean  $\pm$  standard deviation (SD).

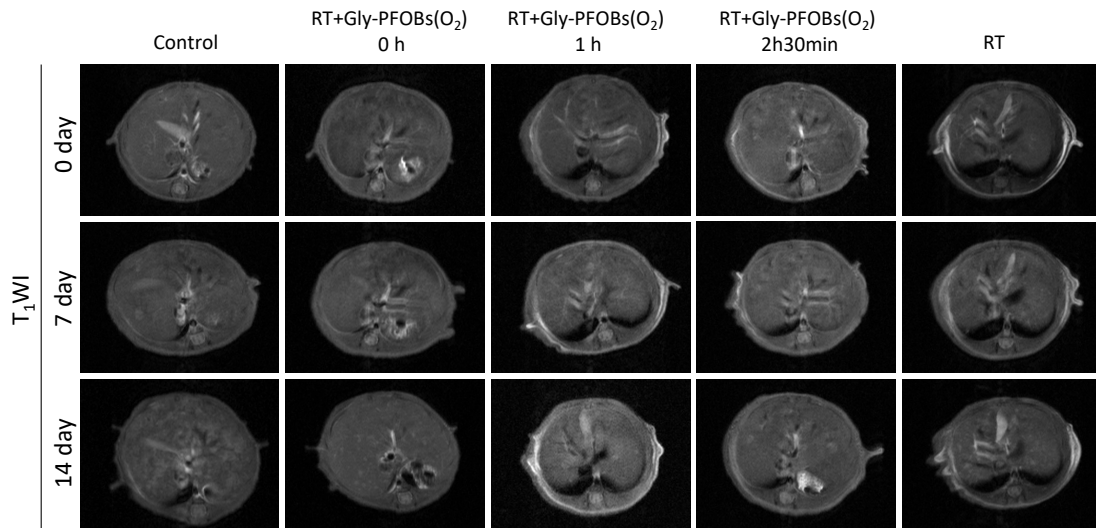


**Supplementary Figure 12. Flow cytometry analysis of cell apoptosis.** a. Determination of apoptosis level of hypoxic NCI-H460 cells co-incubated with Gly-PFOBs (O<sub>2</sub>) probes for different duration of time (0 h, 1~2 h, and 3h) then subjected to X-ray irradiation (6 Gy). b. Corresponding statistical analysis. RT+ Gly-PFOBs 1 h~2 h vs. RT+ Gly-PFOBs 0 h or 3 h,  $P < 0.05$  ( $P = 0.0347$ ); RT+ Gly-PFOBs 1 h~2 h vs. RT alone,  $P < 0.01$  ( $P = 0.0039$ ), \*\*\*\*  $P < 0.0001$ , one-way ANOVA, Tukey's multiple comparisons test,  $n = 4$  independent samples,  $n = 3$  independent samples in Control group. Data are presented as mean  $\pm$  standard deviation (SD). c. Representative gating strategy for the flow cytometry analysis of cell apoptosis. RT: radiotherapy.

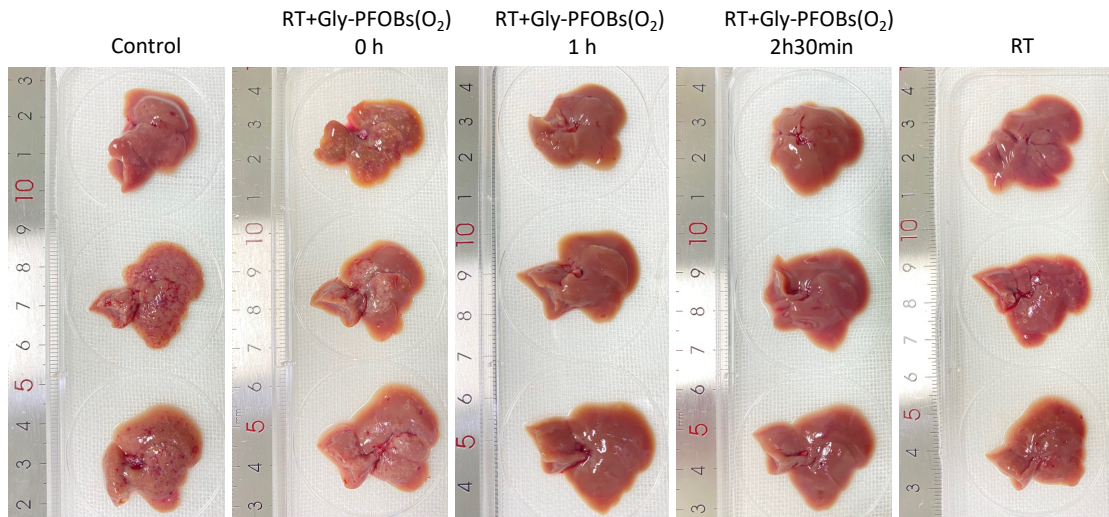




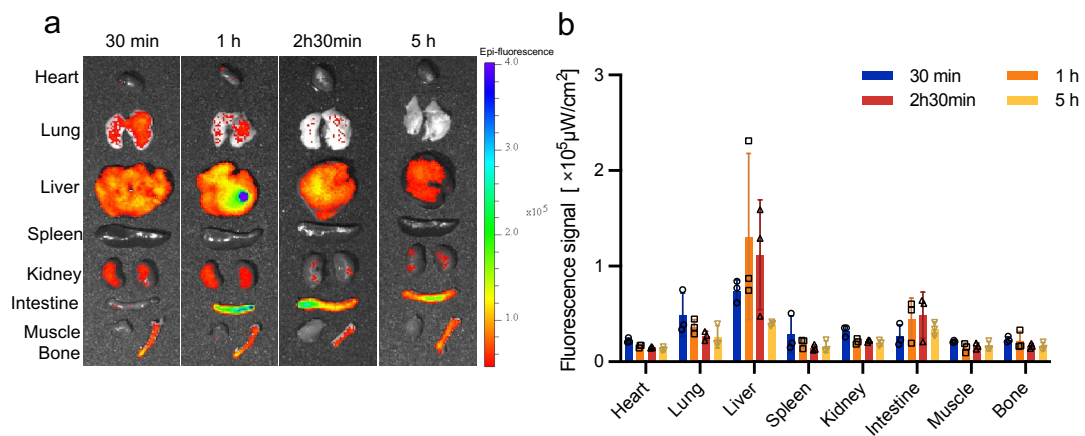
**Supplementary Figure 13. Mouse body weight changes and statistical analysis of immunohistochemical staining.** a. Mouse body weight changes during treatments, n = 4 mice per group. b-d. Statistical results of CD31 (b), Ki67 (c), and TUNEL (d) antigen staining in NCI-H460 subcutaneous tumor of different treatment groups. \*\*\*\*  $P < 0.0001$ , one-way ANOVA, Tukey's multiple comparisons test, n = 5 independent samples. Data are presented as mean  $\pm$  standard deviation (SD). RT: radiotherapy.



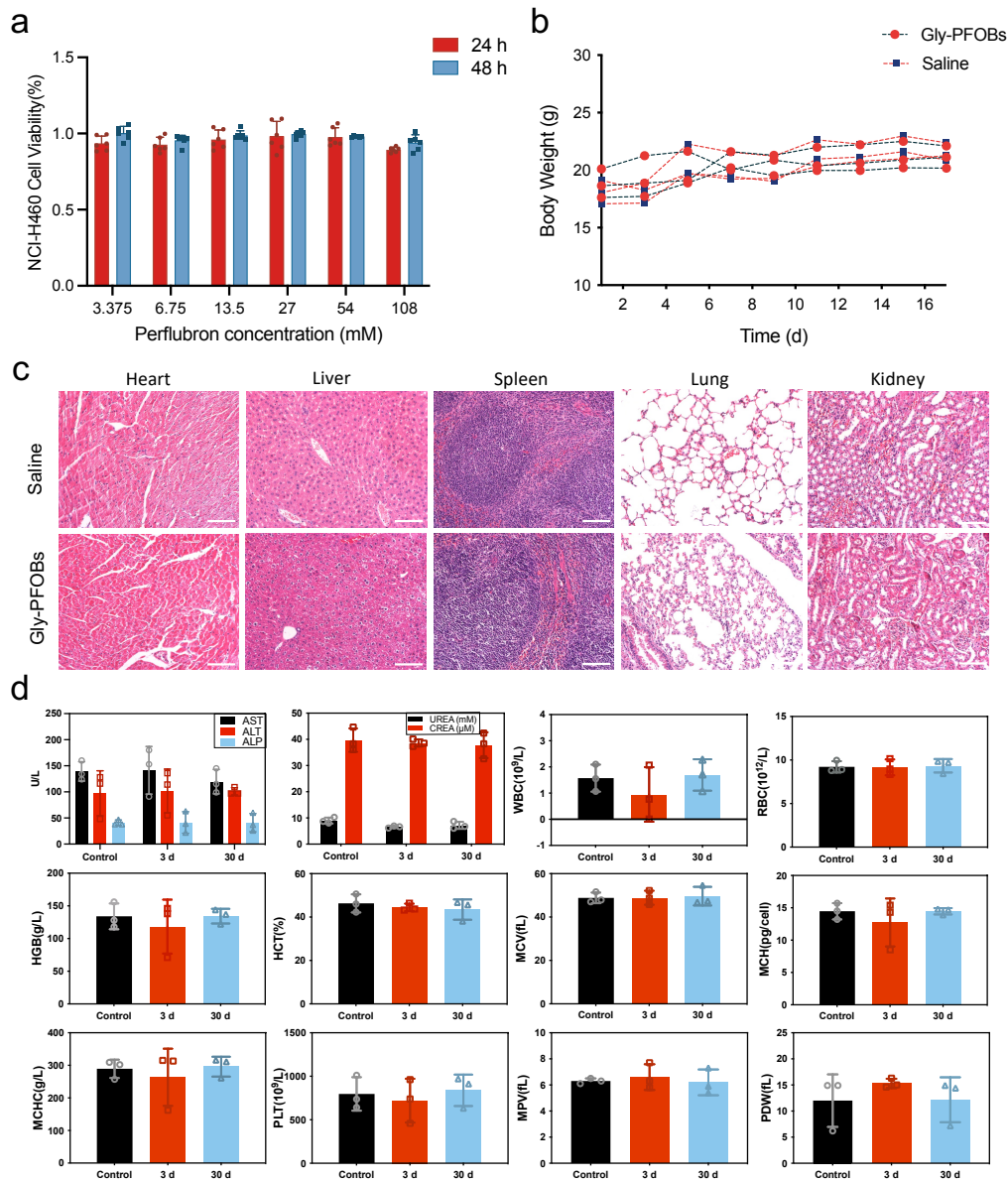
**Supplementary Figure 14.** T<sub>1</sub> weighted MR images of mice in each treatment group at assigned time points, n=3 mice per group.



**Supplementary Figure 15. Representative livers from each treatment group.** Mice were sacrificed on day 14, and representative livers (n = 3 mice) from the treatment groups are displayed. RT: radiotherapy.



**Supplementary Figure 16. Biodistribution results of Gly-PFOBs after injection.** a. Representative IVIS imaging results of NCI-H209 SCLC liver metastases mouse model after Gly-PFOBs injection. b. Corresponding fluorescence signal analysis. Data are presented as mean  $\pm$  standard deviation (SD) (n = 3 mice per group).



**Supplementary Figure 17. Gly-PFOBs cytotoxicity and biocompatibility assessment.**

**a.** Cell viabilities of NCI-H460 cells after co-incubation with Gly-PFOBs for 24 h and 48 h, n = 6 independent measurements. Data are presented as mean ± standard deviation (SD). **b.** Body weight changes. Data are presented as mean ± standard deviation (SD) (n = 3 mice per group). **c.** H&E staining of main organ sections from BALB/c nude mice after Gly-PFOBs injection, scale bar: 100 μm, n = 3 independent samples. **d.** Corresponding hematological analysis of mice treated with saline or Gly-PFOBs. Data are presented as mean ± standard deviation (SD) (n = 3 independent samples). WBC: white blood cells; RBC: red blood cells; HGB: hemoglobin; HCT: hematocrit; MCV: mean corpuscular volume; MCH: mean corpuscular hemoglobin; MCHC: mean corpuscular hemoglobin concentration; PLT: platelets; MPV: mean platelet volume; PDW: platelet distribution width. Blood samples were collected for hematological analysis on day 3 and day 30 after injection, n = 3 mice per group.